



Impact of aortic valve stenosis on myocardial deformation in different left ventricular levels: A three-dimensional speckle tracking echocardiography study

Johannes Just Hjertaas MD, PhD¹  | Eigir Einarsen MD, PhD¹ | Eva Gerds MD, PhD^{1,2} | Marina Kokorina MD² | Christian Arvei Moen MD, PhD² | Stig Urheim MD, PhD^{1,2} | Sahrai Saeed MD, PhD²  | Knut Matre MSc, PhD¹

¹Department of Clinical Science, University of Bergen, Bergen, Norway

²Department of Heart Disease, Haukeland University Hospital, Bergen, Norway

Correspondence

Johannes Just Hjertaas, Department of Clinical Science, University of Bergen, Postbox 7804, 5020 Bergen, Norway.
Email: johannes.hjertaas@gmail.com

Abstract

Background: Global systolic left ventricular (LV) myocardial function progressively declines as degenerative aortic valve stenosis (AS) progresses. Whether this results in uniformly distributed deformation changes from base to apex has not been investigated.

Methods: Eighty-five AS patients underwent three-dimensional (3D) echocardiography in this cross-sectional study. Patients were grouped by peak jet velocity into mild ($n = 32$), moderate ($n = 31$), and severe ($n = 22$) AS. 3D speckle tracking derived strain, rotation, twist, and torsion were obtained to assess global LV function and myocardial function at the apical, mid, and basal levels.

Results: Global longitudinal strain (GLS) was lower in patients with severe AS ($-16.1 \pm 2.4\%$ in mild, $-15.5 \pm 2.5\%$ in moderate, and $-13.5 \pm 3.0\%$ in severe AS [all $p < .01$]). Peak basal and mid longitudinal strain (LS), basal rotation and twist from apical to basal level followed the same pattern, while peak apical LS was higher in moderate AS compared to severe AS (all $p < .05$). In multivariate analyses, lower GLS was particularly associated with male sex, higher body mass index and peak aortic jet velocity, lower basal LS with higher filling pressure (E/e') and LV mass, lower mid LS with higher RWT and presence of AS symptoms, and lower apical LS with male sex and higher systolic blood pressure, respectively (all $p < .05$).

Conclusion: Using 3D speckle tracking echocardiography reveals regional and global changes in LV mechanics in AS related to the severity of AS, LV remodeling and presence of cardiovascular risk factors.

KEYWORDS

3D echocardiography, aortic valve stenosis, left ventricular function, left ventricular myocardial levels, speckle tracking

Abbreviations: 2D, two-dimensional; 3D, three-dimensional; ABr, apical-basal longitudinal strain ratio; ANOVA, analysis of variance; AS, aortic valve stenosis; BMI, body mass index; CMR, cardiac magnetic resonance; ED, end diastole; EF, ejection fraction; ES, end systole; GLS, global longitudinal strain; LS, longitudinal strain; LV, left ventricular; RWT, relative wall thickness; STE, speckle tracking echocardiography; TAVR, transcatheter aortic valve replacement; VPS, volumes per second.

This is an open access article under the terms of the [Creative Commons Attribution](https://creativecommons.org/licenses/by/4.0/) License, which permits use, distribution and reproduction in any medium, provided the original work is properly cited.

© 2023 The Authors. *Echocardiography* published by Wiley Periodicals LLC.

1 | INTRODUCTION

Aortic valve stenosis (AS) progression leads to chronic left ventricular (LV) pressure overload. Initially, the LV adapts with changes in LV geometry and hypertrophy to maintain wall stress and cardiac output.^{1,2} Over time, the LV eventually decompensates, which leads to LV systolic and diastolic dysfunction, myocardial oxygen supply–demand mismatch, ischemia, myocardial fibrosis and eventually symptoms.^{3–5} Myocardial strain is related to the extent of myocardial fibrosis,⁶ and global longitudinal strain (GLS) assessed by two-dimensional (2D) and three-dimensional (3D) speckle tracking echocardiography (STE) may detect subclinical systolic dysfunction before changes in ejection fraction (EF) occur.^{6–11} Nevertheless, in AS, changes in longitudinal function may occur in different LV levels that are not captured by looking at the LV as a whole.⁷ Reduced basal longitudinal strain (LS) by 2D STE have been shown to be a more sensitive marker than GLS in predicting outcome in AS.¹²

However, LV deformation occurs not only in the longitudinal direction, but in three dimensions, and is dependent on LV twist and rotation for efficient cardiac contraction and relaxation.^{13,14} Although 2D STE echocardiography may be used to measure rotation and twist, this method has several limitations, such as losing speckles from out-of-plane motion.^{15–17} 3D STE, on the other hand, has better accuracy, reproducibility, and may overcome the limitations of 2D STE.¹⁸ In patients with AS, a few smaller studies using 2D and 3D echocardiography have shown increased apical rotation in severe AS.^{19–21} However, there is still limited knowledge from 3D STE on how AS severity impacts myocardial deformation in different LV levels. Accordingly, the present study aims to explore the impact of AS severity on strain and twist measurements in different levels of the LV using 3D STE.

2 | METHODS

2.1 | Study population

This cross-sectional study recruited patients from the outpatient clinic at Haukeland University Hospital, Bergen, Norway, who underwent serial echocardiographic examinations to follow progression of degenerative AS. Exclusion criteria were known coronary artery disease, previous cardiothoracic surgery, TAVR, coexisting aortic regurgitation, or other known valve diseases that could affect deformation values in any direction, based on hospital medical records. Patients with known atrial fibrillation were excluded based on the requirement of a regular heart rhythm to use 3D stitched images without artifacts. In addition, patients with known image quality too poor to be analyzed were excluded retrospectively.

Of 120 patients included, 7 were excluded because of irregular heart rate, 1 because of previously unknown myocardial infarction, and 27 patients due to poor image quality or volume stitching artifacts which precluded 3D STE analysis. This resulted in 85 patients eligible for the present analysis.

The study was approved by the Norwegian regional committee for medical health and research ethics (2014/1895/REK Nord). All patients gave written informed consent. Self-reported information on medical history, cardiovascular risk factors and medication treatment was collected on a standardized questionnaire, and data were quality assured by study personnel. A 12-lead electrocardiogram and brachial blood pressure measurement both before and after the echocardiogram were undertaken in all patients by a study nurse.

2.2 | Echocardiography

A standardized imaging protocol for 2D and 3D echocardiography using a Vivid E9 scanner with M5S probe (GE Vingmed Ultrasound AS, Horten, Norway) for 2D imaging, and 4 V probe for 3D imaging (GE Vingmed Ultrasound AS, Horten, Norway) was applied in all patients. Volume-stitched 3D images were obtained using six beats with a target volume rate of 35 volumes per second (VPS) using harmonic imaging, as these were the optimal settings for deformation measurements found in previous in-vitro studies.^{22,23} The sector width was adjusted as narrowly as possible, while still covering the entire LV, optimized for post processing STE analysis. Patients were instructed to hold their breath during recording of two, four, and six heart cycles. To ensure quality, multiple 3D recordings were acquired.

2.3 | Echocardiographic measurements

Conventional 2D echocardiographic images were analyzed using ImageArena (TomTec Imaging Systems, GmbH, Unterschleissheim, Germany). LV quantification was performed following the joint European Association of Cardiovascular Imaging (EACVI) and American Society of Echocardiography (ASE) guidelines.²⁴ AS severity was assessed by peak jet velocity, mean aortic gradient, and aortic valve area using the continuity equation.^{25,26} EF was estimated using bi-plane method of disks. Filling pressure was estimated from ASE/EACVI diastolic function guidelines using the ratio of peak early transmitral blood velocity to average early mitral annular velocity (E/e').²⁷ All 2D echocardiograms were initially read by a single investigator (E.E) and later proofread by an experienced reader (E.G.).

3D STE data were analyzed using EchoPAC v202 (GE Vingmed Ultrasound AS, Horten, Norway). The best 3D recordings were selected using multi-slice short axis view, to ensure optimal image quality and to avoid images with any stitching artifacts. STE was analyzed by the software's 4D Auto LVQ-tool (Figure 1A & 1B). For this process, the LV in the three apical views from 3D were manually aligned with the axial axis. The apex and mid base were manually defined at both end-diastole (ED) and end-systole (ES) before the software automatically tracked the LV lumen. Any tracking inaccuracies were manually corrected. Any segment with tracking errors or artifacts was rejected. If the software was unable to track more than three segments, the

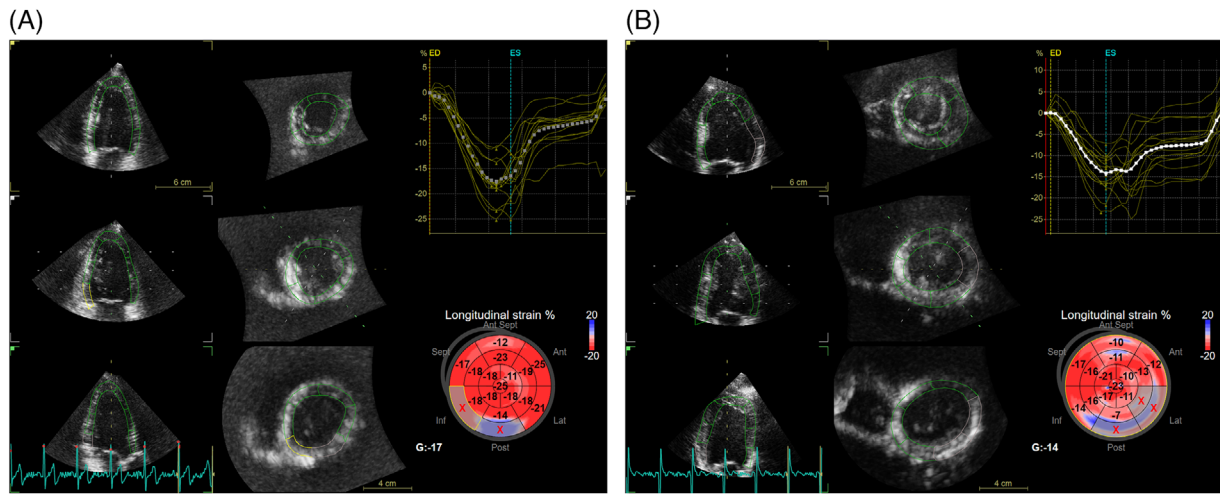


FIGURE 1 3D views of the LV. Example of 3D echocardiographic image in patients with mild (A) and severe (B) AS with corresponding LS curves and bull's-eye plot.

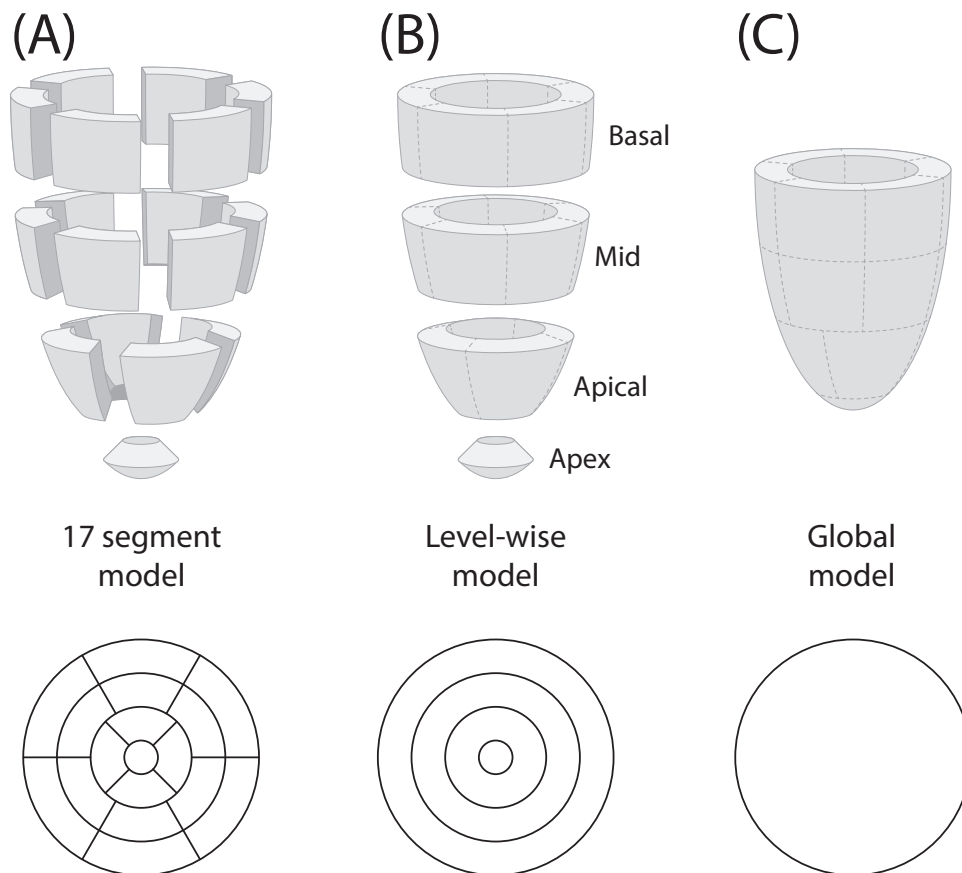


FIGURE 2 Segmentation models. Regional segmentation models of the left ventricle. Standard 17 segment model with bull's-eye plot (A). Segmentation by basal, mid, apical and apex levels (B). Global model (C).

recording was considered of poor image quality, and the patient was excluded. The software then calculated the LV 3D volumes and timing of ED and ES from the minimum and maximum LV-volume. The software then tracked the epicardial border at ES and ED. Any mismatches were manually corrected.

2.4 | Data analysis

3D STE analysis was performed in a standard LV model with 17 segments (Figure 2A). This model consists of six basal, six mid, and four apical segments as well as one segment for the apex.²⁴ The EchoPAC

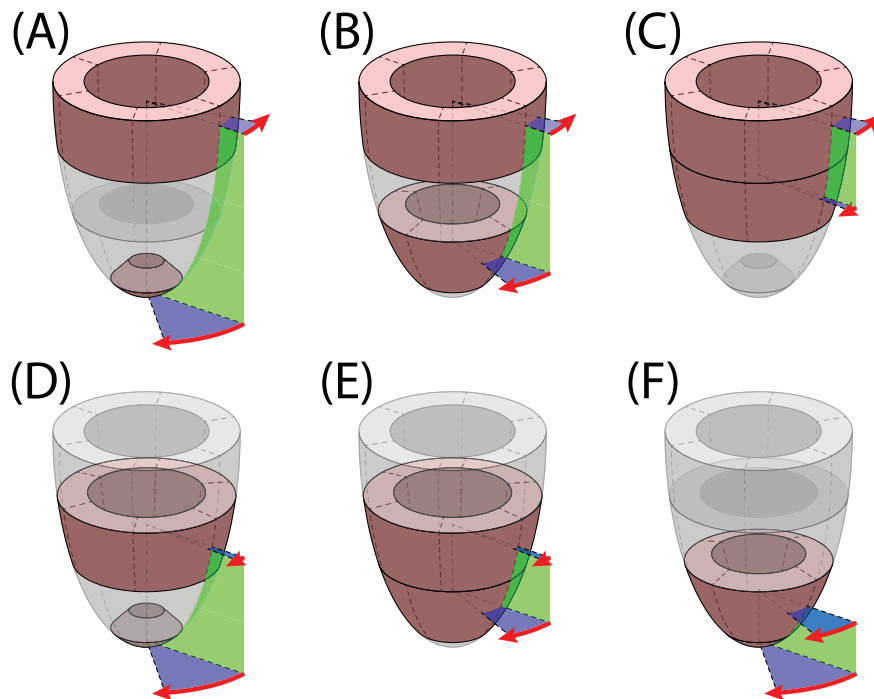


FIGURE 3 Rotation by levels. Level combinations used for twist calculation. Apex-basal or global twist (A), apical-basal twist (B), mid-basal twist (C), apex-mid twist (D), apical-mid twist (E), and apex-apical twist (F).

software also provided 3D STE-derived rotation curves for the basal, mid, apical, and apex levels of the LV relative to the ultrasound probe (Figure 2B). Twist, which is defined as the difference in rotation between two different planes, was provided by the software, and found to be identical with basal rotation subtracted from apex rotation (Figure 3A). Torsion is defined as twist divided by the distance between the two planes, and was provided for the basal, mid, and apical LV levels. Average 3D strain in longitudinal, circumferential, and radial direction as well as area strain was calculated for each LV level using a custom written Python program running Python 3 (Python Software Foundation, Wilmington, Delaware, USA). The global twist provided from the EchoPAC software was identical to The Python program also calculated twist for the six possible combinations [basal-apex (Figure 3A), basal-apical (Figure 3B), basal-mid (Figure 3C), mid-apex (Figure 3D), mid-apical (Figure 3E), and apical-apex (Figure 3F)]. Apical-basal longitudinal strain ratio (ABr) was calculated by dividing the mean LS of the four apical segments by the mean six basal segments.

Negative peak values for longitudinal, circumferential, area strain, and positive peak values for radial strain were recorded for both regional (Figure 2B) and global (Figure 2C) curves. Positive peak rotation values were registered for the apex, apical and mid-levels, while negative peak rotation values were registered in the basal level. Peak negative twist rate was registered as peak untwist.

2.5 | Statistics

Statistical analysis was conducted using R version 3.5.1 (The R Foundation for Statistical Computing, Vienna, Austria) and SPSS version 25 (SPSS Inc., Chicago, Illinois, USA).

The population was divided into AS severity classes based on peak aortic jet velocity: mild AS (< 3.0 m/s), moderate AS (3.0 – 3.9 m/s),

and severe AS (≥ 4.0 m/s).^{25,26} Results are presented as mean \pm standard deviation. One-way analysis of variance (ANOVA) with Bonferroni post hoc test was used to show any difference between the groups for continuous variables.

Comparison of strain, rotation and torsion between different myocardial levels, was performed using mixed two-way ANOVA, with AS severity as group factor (P_g) and LV level as within-factor (P_w). Post hoc Bonferroni contrasts were used when appropriate. The Greenhouse-Geisser adjustment of freedom was used for evaluation of the main effect when Mauchly's test of sphericity was violated.

Uni- and multivariable linear regression was used to identify any covariables. 3D STE and LS at different levels were used as dependent variables while relative wall thickness (RWT), Peak jet velocity, E/e' , LV mass, sex, symptoms, and body mass index (BMI) were used as independent variables. For LS, multivariable linear regression using a stepwise procedure was first used to identify covariates, and then systolic BP and sex were forced into all models. Results were reported as standardized beta coefficients.

Intra- and interobserver variability was assessed by re-analyzing 20 randomly selected patients in a blinded manner and reported as intraclass correlation coefficient (ICC) and mean difference between the results.

3 | RESULTS

3.1 | Patient characteristics

The total study cohort included 32 patients with mild, 31 with moderate, and 22 with severe AS (Table 1). While most patients were

TABLE 1 Patient and 2D echocardiographic characteristics.

Variable	All patients (n = 85)	Mild AS (n = 32)	Moderate AS (n = 31)	Severe AS (n = 22)	One-way ANOVA
Age (years)	72 ± 12	71 ± 10	71 ± 14	75 ± 10	.393
Sex (male)	44 (51%)	15 (45%)	18 (58%)	11 (50%)	.533
Weight (kg)	75 ± 15	76 ± 12	77 ± 17	72 ± 15	.582
Height (cm)	170 ± 9	169 ± 9	171 ± 9	170 ± 9	.475
BMI (kg/m ²)	26.0 ± 3.2	26.6 ± 3.7	26.0 ± 4.5	25.1 ± 3.4	.392
BSA (m ²)	1.86 ± .21	1.85 ± .18	1.89 ± .24	1.83 ± .22	.617
Symptoms (≥ NYHA2)	13	0	6	7 ^a	.004
Heart rate (beats/min)	68 ± 10	66 ± 9	67 ± 9	72 ± 13	.143
Systolic BP (mmHg)	149 ± 23	153 ± 27	144 ± 21	148 ± 18	.264
Diastolic BP (mmHg)	83 ± 9	83 ± 11	83 ± 8	82 ± 9	.933
Current smokers (%)	7	3	10	9	.574
Diabetes (%)	8	13	10	0	.247
Hypertension (%)	87	88	90	82	.667
Peak aortic jet velocity (m/s)	3.41 ± .89	2.50 ± .27	3.50 ± .25 ^a	4.60 ± .44 ^{a,b}	<.001
Mean aortic Gradient (mmHg)	27.0 ± 15.2	13.4 ± 3.4	26.0 ± 4.0 ^a	48.2 ± 11.3 ^{a,b}	<.001
Aorta valve area (cm ²)	1.39 ± .50	1.88 ± .34	1.23 ± .30 ^a	.92 ± .19 ^{a,b}	<.001
LVEF (%)	62 ± 5	63 ± 4	62 ± 5	63 ± 7	.397
IVSd (cm)	1.34 ± .30	1.27 ± .22	1.27 ± .31	1.54 ± .30 ^{a,b}	<.001
LVIDd (cm)	4.67 ± .62	4.70 ± .59	4.70 ± .57	4.59 ± .73	.791
PWDd (cm)	1.00 ± .18	.94 ± .12	.99 ± .20	1.09 ± .22 ^a	.013
E/e'	12.28 ± 4.41	1.47 ± 3.03	12.65 ± 4.84	14.31 ± 4.58 ^a	.005
RWT	.43 ± .09	.40 ± .08	.42 ± .09	.48 ± .10 ^a	.017

Data are mean ± SD.

Abbreviations: AS, aortic valve stenosis; ANOVA, analysis of variance; BMI, body mass index; BSA, body surface area; BP, blood pressure; E/e', filling pressure; IVSd, septum thickness at end diastole; LVEF, left ventricle ejection fraction; LVIDd, left ventricle internal diameter at end diastole; PWDd, posterior wall thickness at end diastole; RWT, relative wall thickness.

^aDifference with mild AS.

^bDifference with moderate AS.

asymptomatic, 13 reported dyspnea (New York Heart Association functional class II-III) in the questionnaire, 6 in the moderate AS, and 7 in the severe AS group. None reported angina pectoris or syncope. The E/e' ratio and RWT were higher in patients with severe AS ($p = .017$), while sex, age, BMI, and blood pressure did not differ (Table 1).

3.2 | 3D echocardiography

3.2.1 | Longitudinal strain

GLS was significantly lower in severe AS patients compared to mild and moderate AS ($p = .002$) (Table 2 and Supplementary figure 1). Basal and mid LS followed a parallel pattern with lower values in the severe than mild AS group ($p < .001$ and $p = .004$ for basal and mid, respectively) (Table 3). Apical LS was lower in the severe than moderate AS group ($p = .027$), while mild AS did not differ significantly from either (Figure 4A).

3.2.2 | Circumferential strain

Global circumferential strain (GCS) showed no difference between the groups of AS severity. Circumferential level strain was highest in the apical level in all AS severity groups, but no difference was found between the AS severity groups.

3.2.3 | Area strain

Area level strain was higher in the apical than in the basal level. Both mid and basal levels showed lower area strain for severe than mild AS.

3.2.4 | Radial strain

Radial strain was higher in the apical than basal level for the moderate and severe AS groups and was lower in severe than mild AS for mid and basal level.

TABLE 2 3D STE characteristics.

Variable	Mild AS (n = 32) (A)	Moderate AS (n = 31) (B)	Severe AS (n = 22) (C)	One-way ANOVA
Volume rate (VPS)	36.2 ± 4.1	36.0 ± 7.7	34.3 ± 1.8	.405
Peak Global Strain (%)				
Longitudinal	-16.1 ± 2.4	-15.5 ± 2.5	-13.5 ± 3.0 ^{ab}	.002
Circumferential	-17.1 ± 3.6	-17.1 ± 3.8	-16.5 ± 4.7	.808
Area	-29.0 ± 4.1	-28.6 ± 4.3	-26.1 ± 5.3	.052
Radial	47.4 ± 11.3	46.9 ± 11.0	41.9 ± 11.7	.172
Peak Twist (°)				
Apex-Basal (Global)	9.0 ± 5.5	11.8 ± 5.4	12.1 ± 6.5	.079
Apex-Mid	7.1 ± 5.1	4.5 ± 3.4	3.5 ± 4.4	.255
Apex-Apical	3.1 ± 3.3	9.2 ± 4.5	8.4 ± 6.0	.324
Apical-Basal	7.0 ± 2.8	7.8 ± 3.5	10.1 ± 3.1 ^{ab}	.003
Apical-Mid	4.8 ± 1.9	5.0 ± 2.3	6.0 ± 2.2	.100
Mid-Basal	2.4 ± 1.7	2.9 ± 1.9	4.1 ± 1.6 ^a	.003
Peak untwist (° · s ⁻¹)				
Apex-Base (Global)	-101.9 ± 54.8	-109.2 ± 40.8	-110.6 ± 43.8	.758
Apex-Mid	-87.5 ± 49.4	-94.9 ± 33.0	-84.8 ± 39.5	.646
Apex-Apical	-63.6 ± 37.5	-63.6 ± 22.6	-52.1 ± 24.3	.297
Apical-Basal	-61.4 ± 26.4	-63.2 ± 25.5	-87.1 ± 29.9 ^{ab}	.002
Apical-Mid	-36.7 ± 19.1	-40.6 ± 19.3	-53.0 ± 20.6 ^a	.012
Mid-Basal	-34.3 ± 12.0	-34.9 ± 11.9	-42.2 ± 14.1	.054
ABr	.82 ± .24	1.00 ± .30 ^a	.92 ± .21	.015
Global Torsion (° · cm ⁻¹)	1.8 ± .8	2.1 ± .9	2.3 ± 1.0	.138
LV Mass (g)	153 ± 38	165 ± 38	169 ± 60	.363
GCS/GLS ratio	1.08 ± .22	1.11 ± .22	1.26 ± .37	.053

Data are mean ± SD.

Abbreviations: ABr, apical-basal longitudinal strain ratio; AS, aortic valve stenosis; ANOVA, analysis of variance; GCS, global circumferential strain; GLS, global longitudinal strain; LV, left ventricle; STE, speckle tracking echocardiography; VPS, volumes per second.

^a*p* < .05 vs. Mild AS group.

^b*p* < .05 vs. Moderate AS group.

3.2.5 | Rotation

Peak rotation, presented in Table 3, showed a gradient in rotation from base towards apex with positive rotation (counterclockwise) at apex level and negative rotation (clockwise) at the basal level during systole, when observed from the apex. There was a significant difference between each level except between the apex and apical level, which only differed in the moderate AS group. Between the groups, basal rotation was significantly higher in severe AS (Figure 4B and Supplementary figure 2).

3.2.6 | Twist

Peak twist increased with AS severity for apical-basal and mid-basal twist (Table 2 and Supplementary figure 3). Peak untwist was

higher in patients with severe AS for Apical-Basal and Apical-Mid untwist.

3.2.7 | Torsion

Although global torsion showed borderline significance between the severity groups, there was no difference in torsion by severity for different levels (Table 3).

3.3 | Covariate analysis

Using multivariable linear regression analysis in the total study population, partially different independent covariates of 3D STE GLS and LS at basal, mid, and apical level were identified (Table 4). Lower GLS was

TABLE 3 3D STE strain, rotation, and torsion at different LV levels.

	Mild AS (n = 32) (A)	Moderate AS (n = 31) (B)	Severe AS (n = 22) (C)	Two-way mixed ANOVA
Longitudinal strain (%)				
Apex	n.a.	n.a.	n.a.	$p_w < .001, p_g < .001, p_i = .029$
Apical	-14.9 ± 3.8	-16.1 ± 3.4	-13.4 ± 3.2^b	
Mid	-15.3 ± 3.6	$-14.1 \pm 3.1^{**}$	-12.2 ± 3.2^a	
Basal	$-18.7 \pm 3.2^{***}$	$-16.7 \pm 3.6^{**}$	$-14.9 \pm 3.8^{a,***}$	
Circumferential strain (%)				
Apex	n.a.	n.a.	n.a.	$p_w < .001, p_g = .767, p_i = .493$
Apical	-19.6 ± 5.6	-19.6 ± 5.6	-19.9 ± 7.1	
Mid	$-17.0 \pm 2.4^{**}$	$-16.8 \pm 4.6^{**}$	$-15.8 \pm 4.3^{**}$	
Basal	$-13.4 \pm 3.4^{***}$	$-13.1 \pm 3.4^{***}$	$-12.0 \pm 3.5^{***}$	
Area strain (%)				
Apex	n.a.	n.a.	n.a.	$p_w < .001, p_g = .031, p_i = .117$
Apical	-30.3 ± 6.3	-31.1 ± 5.6	-29.2 ± 7.0	
Mid	-28.7 ± 3.5	$-27.4 \pm 5.7^{**}$	$-24.9 \pm 5.5^{a,***}$	
Basal	-28.0 ± 4.2	$-26.2 \pm 4.6^{**}$	$-23.4 \pm 5.0^{a,***}$	
Radial strain (%)				
Apex	n.a.	n.a.	n.a.	$p_w < .001, p_g = .266, p_i = .078$
Apical	50.8 ± 17.3	53.1 ± 17.6	48.7 ± 17.4	
Mid	$43.5 \pm 7.6^{**}$	$41.6 \pm 11.1^{**}$	$36.0 \pm 11.3^{a,***}$	
Basal	44.3 ± 8.7	$41.1 \pm 8.5^{**}$	$35.0 \pm 10.2^{a,***}$	
Rotation (°)				
Apex	7.3 ± 5.3	9.7 ± 5.2	9.1 ± 6.1	$p_w < .001, p_g = .150, p_i = .098$
Apical	5.4 ± 2.2	$6.3 \pm 3.1^*$	7.1 ± 3.1	
Mid	$1.1 \pm 1.4^{***}$	$1.8 \pm 1.6^{**}$	$1.8 \pm 1.8^{***}$	
Basal	$-2.0 \pm 1.9^{***}$	$-1.8 \pm 1.5^{***}$	$-3.2 \pm 1.9^{a,b,***}$	
Torsion (°·cm⁻¹)				
Apex	n.a.	n.a.	n.a.	$p_w < .001, p_g = .138, p_i = .470$
Apical	2.2 ± 1.6	3.1 ± 1.6	2.7 ± 2.3	
Mid	2.3 ± 1.1	2.2 ± 1.2	$2.7 \pm .9$	
Basal	$.7 \pm .6^{**}$	$.8 \pm .8^{**}$	$1.1 \pm 1.1^{***}$	

Data are mean \pm SD.

Abbreviations: ANOVA, analysis of variance; V, left ventricle; STE, speckle tracking echocardiography; Pw, Pg, and Pi, *p*-values for within-subjects (level), between-groups (severity), and interaction from two-way mixed ANOVA, respectively.

^a*p* < .05 vs. Mild AS group

^b*p* < .05 vs. Moderate AS group

**p* < .05 vs. Apex level

***p* < .05 vs. Apical level

****p* < .05 vs. Mid level

particularly associated with male sex, higher BMI, and higher peak aortic jet velocity. Furthermore, lower basal LS was associated with higher filling pressure (E/e') and higher LV mass. Lower mid LS was independently associated with higher RWT and presence of symptoms. Lower

apical LS was associated with male sex and higher systolic blood pressure (all *p* < .05). Increased apical-basal twist was associated with higher RWT, higher E/e', higher peak jet velocity, higher BMI, lower GCS, but not with symptoms (Table 5).

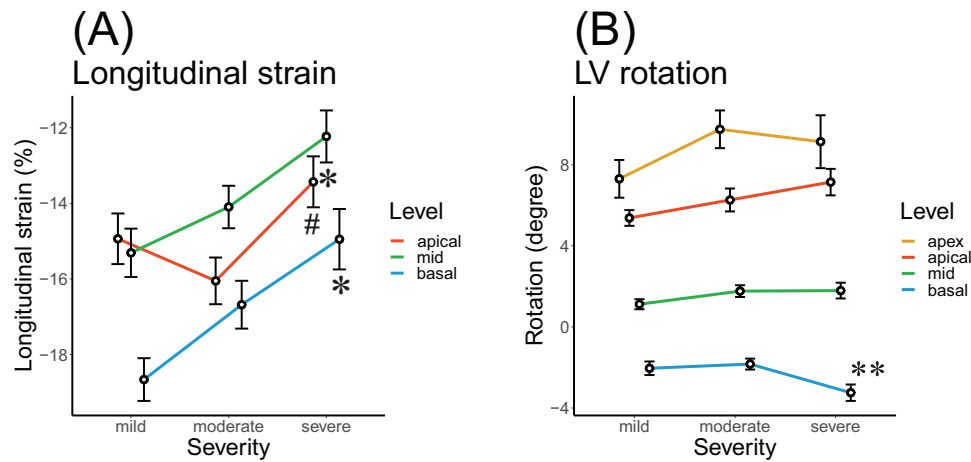


FIGURE 4 Longitudinal strain and LV rotation by severity and LV level. Longitudinal strain at apical, mid, and basal level (A); Left ventricular rotation at apex, apical, mid, and basal level (B). Vertical lines represent standard error of mean; * $p < .05$ vs. Mild AS group; ** $p < .05$ vs. Moderate AS group.

TABLE 4 Univariate and multivariate association of longitudinal strain in different levels and GLS.

Dependent variables	Global longitudinal strain		Basal longitudinal strain		Mid longitudinal strain		Apical longitudinal strain									
	Univariate		Multivariate ^a		Univariate		Multivariate ^a									
	β	p	β	p	β	p	β	p								
RWT	.330	.002			.189	.084			.402	<.001	.358	<.001	.173	.113		
Peak jet velocity (m/s)	.405	<.001	.383	<.001	.381	<.001	.196	.069	.384	<.001			.195	.074		
E/e'	.143	.193			.276	.011	.252	.018	.135	.220			-.050	.654		
LV mass (g)	.473	<.001			.465	<.001	.271	.031	.327	.002	.191	.118	.294	.006		
Sex (male)	.427	<.001	.334	.001	.293	.007	.149	.241	.290	.007	.093	.452	.397	<.001	.437	<.001
Age	.038	.729			.039	.726			.033	.817			.084	.447		
Symptoms (\geq NYHA2)	.346	.001			.220	.043			.328	.002	.236	.018	.261	.016		
BMI	.287	.008	.268	.006	.131	.233			.164	.133			.324	.002		
Systolic BP (mmHg)	.013	.212	-.085	.371	-.033	.765	-.020	.840	.032	.772	.066	.493	-.281	.009	-.343	.001

Abbreviations: BMI, body mass index; BP, blood pressure; E/e', filling pressure; LV, left ventricle; RWT, relative wall thickness.

^aStepwise multivariate modeling with additional forced variables (sex and systolic BP).

TABLE 5 Covariates of apical-basal twist in uni- and multivariable linear regression analyses.

Model multiple R^2	Univariable		Multivariable Model 1		Multivariable Model 2	
	Beta	p	Beta	p	Beta	p
Model multiple R^2			Multiple R^2 .480, $p < .001$		Multiple R^2 = .482, $p < .001$	
Dependent variables						
RWT	.243	.025	.212	.020	.216	.018
E/e'	.454	<.001	.228	.015	.227	.015
Peak jet velocity (m/s)	.357	<.001	.219	.023	.200	.049
GCS (%)	-.479	<.001	-.427	<.001	-.443	<.001
BMI	-.357	<.001	-.146	.106	-.146	.106
Symptoms (\geq NYHA2)	.022	.843			.054	.563

Abbreviations: BMI, body mass index; E/e', filling pressure; GCS, global circumferential strain; RWT, relative wall thickness.

3.4 | Reproducibility

Inter- and intraobserver variability was excellent for 3D STE data. Reproducibility for 3D strain, rotation, and torsion is presented in Supplementary table 1.

4 | DISCUSSION

The present cross-sectional study using 3D STE gives novel information on the association of AS severity and other clinically important confounders with myocardial deformation at different LV levels. As demonstrated, increasing AS severity is associated with a reduction in LS, particularly in the basal and mid LV level. Other regional myocardial deformation markers like circumferential, radial, and area strain as well as torsion, showed no significant difference. Using 3D STE, apical LS may seem to be preserved in patients with both mild and moderate AS, while patients with severe AS have reduced apical LS. This hints to a possible compensatory role for apical LS in preserving GLS in mild and moderate AS. Furthermore, we found that apical-basal twist was higher in patients with severe AS compared to mild and moderate AS. Our findings expand results from previous studies by 2D STE, demonstrating GLS to be reduced with increasing severity,^{7,8} and lower basal LS in symptomatic AS²⁸ by revealing that regional and global changes in LV mechanics in AS are not only related to the severity of AS, but also to LV remodeling and presence of cardiovascular risk factors in the individual patient.

Schueler et al. were the first to explore the feasibility and usefulness of 3D strain for the determination of changes in LV mechanics after transcatheter aortic valve implantation (TAVR).²⁹ In their study, 44 elderly patients underwent 2D and 3D LV deformation imaging before, and 6 months after TAVR. The authors showed that 3D LS significantly increased 6 months after TAVR, while no significant changes were observed in twist and rotation, or 2D strain. Of note, 3D strain values at basal and apical LV levels were not reported.

Several studies have shown that rotation and twist is higher in patients with more severe AS.^{19,20,30} Using 2D STE, Holmes et al. found increased apical rotation to be associated with poor survival in severe AS, suggesting apical rotation as a compensatory mechanism to preserve cardiac output in severe LV outflow obstruction.¹⁹ In the present study, only basal rotation was higher in the severe AS group. This could possibly be explained by the nature of a twisting object, where the middle part has close to stationary rotation, if the two ends rotate the same amount in opposite directions. However, the apex rotation showed much wider dispersion than the other levels of rotation in the present study, reflecting 3D STE measurement limitations involving the apex. Our findings of increased basal rotation contrasts with a smaller 2D STE study by van Dalen et al.,³⁰ which reported similar basal rotation in 24 normal controls and 48 patients with AS. The same study also found significantly higher apical rotation and twist in patients with AS than control subjects.

The present study compared six different combinations of twist measurement. Ideally twist would be measured from apex to the basal

level. Because of the apex rotation dispersion, twist involving apex also showed much wider dispersion than for other twist combinations. Twist measured one level down, from apical to basal level, gave much less dispersion. Comparison of apical-basal twist between the groups also showed a significant increase in twist for the severe AS group, while none of the twist combinations involving the apex showed any significant difference between the groups. Although not found in this study, a potential loss of apical function in severe AS could also affect apical rotation, which has been reported in symptomatic AS patients.³¹ LV rotation, however, may not be considered a strict deformation parameter, as it is relative to the observer, namely, the probe. LV twist and torsion, on the other hand, can be considered as true deformation parameters, as their relative measurements are both within the myocardium.

Interestingly, diverse clinical and echocardiographic covariates of 3D STE LS were identified at different levels, expanding previous knowledge from 2D STE studies assessing covariates of GLS in AS. Peak jet velocity and LV mass were identified as determinants of GLS but also of basal LS, and RWT as determinant of mid-level LS.^{7,8,32} In a prospective study of 220 patients with severe asymptomatic AS, higher LV mass index was associated with impaired GLS.³³ In that study, neither GLS nor LV mass index differed between groups of patients that developed symptoms during follow-up. In the present cross-sectional 3D study, presence of symptoms was associated with reduced LS at the mid-level. In addition, male sex was a major determinant of GLS and apical LS, as previously reported from a 2D study.⁷ In contrast to the findings of Ng et al. we found no association between age and GLS or LS at any level.⁸ Higher RWT was associated with lower mid LS, but not with lower GLS, as previous reported in a 2D STE study by Dahl et al.³² In addition, higher body mass index was independently associated with lower 3D GLS, expanding findings in a 2D STE study in 44 patients with severe AS that found obesity to be associated with lower GLS and with more endomyocardial fibrosis in endocardial biopsies.³⁴

4.1 | Clinical implications

As a clinical tool, 3D STE strain, twist and other parameters related to LV mechanics have the potential to identify subclinical dysfunction as well as monitor disease progression and response to treatment. In a recent survey conducted by the EACVI,³⁵ it was shown that > 90% of European echo labs had access to 3D echocardiography, but the majority of centers reserved the technique for selected cases and specific indications. The most frequent use was assessment of LV dimensions and function before cardiac device implantation or surgery for valvular heart disease, or as screening for cardiotoxicity from chemotherapy. AS is the most common valvular heart diseases requiring valve replacement or intervention and the incidence is increasing. The optimal timing of intervention for asymptomatic patients is challenging. Hence, the assessment of LV function by 3D LV deformation has potential as a valuable supplement to the routine follow-up of AS patients who have normal conventional EF and are apparently asymptomatic. The present

study suggests that basal LS may be important as an early marker of LV deterioration in patients with AS and EF > 50%.

4.2 | Limitations

One of the main limitations of 3D STE compared to 2D is its lower temporal resolution. It can be argued that the extra added dimension reduces the need for a high temporal resolution due to the ability to track speckles in all directions and follow the speckles in 3D space.^{15,22,36} However, if the volume rate becomes too low, measurements and peaks may be underestimated. For the same reason, the usefulness of time derivative on 3D STE deformation to produce strain rate and twist rate is limited. Assessment of time to untwist was not included in the present analysis for this reason. This study used a volume rate of 36 ± 6 , which was considered an optimal volume rate for 3D STE in our previous in vitro studies,^{22,23} and gave good reproducibility of 3D strain and twist against sonomicrometry as a gold standard. The low temporal resolution makes measurements dependent on curve derivation, such as strain rate and untwist rate, unreliable, and peak values will be inaccurate.

Of the 120 patients initially enrolled, only 70% were included in the final study, mostly because of poor 3D STE tracking. This was mainly due to poor acoustic visibility and stitching artifacts, which may limit the use of 3D STE in clinical practice.

The present study was not designed to compare 3D STE versus 2D STE, but rather to explore 3D STE findings. Furthermore, the study did not include a healthy control group without AS.

The patient population in this study was not screened for transthyretin cardiac amyloidosis (ATTR-CM). Studies in the later years have shown ATTR-CM to be much more abundant than previously anticipated, especially in the AS population, where some studies have shown ATTR-CM to be prevalent in up to 16%,³⁷ especially in those with the subgroup of low-flow, low-gradient AS.³⁸ As ATTR-CM is known to affect basal LS with apical sparing,³⁹ it cannot be excluded that our findings of reduced basal strain with preserved apical strain may have been confounded by ATTR-CM.

Although few studies have explored level-specific deformation in AS by 3D STE, high apical to basal LS ratio has been associated with poorer outcome in two previous studies using 2D STE.^{40,41}

Inter-vendor difference for 3D strain measuring has been reported,⁴² and our results should therefore not be extrapolated to other vendors. Since twist planes may be placed at different levels of the LV by different 3D STE algorithms, twist measurements are particularly vulnerable to inter-vendor differences.

Of clinical importance, the presence of symptoms in our cohort was based on patient self-reports, and systematic exercise testing was not included in this protocol. Lack of physical activity, especially in the aging group of patients, could mask apparent symptoms.

Our participants did not undergo cardiac magnetic resonance (CMR). Earlier CMR studies using myocardial tagging and feature tracking imaging have demonstrated normal values from deformation measurements in different myocardial levels and myocardial

layers.^{43,44} However, the use of CMR is more resource demanding and less available compared to echocardiography.

5 | CONCLUSION

This study shows that 3D STE can reveal regional and global changes in LV mechanics related to the severity of AS, LV remodeling, and cardiovascular risk factors. Patients with severe AS had lower GLS and higher apical-basal twist than those with mild and moderate AS.

When looking at regional deformation of LV levels, deformation changes seem to be more prevalent in the basal LV levels. Apical level LS tends to have a biphasic pattern with higher ABr for moderate than mild AS, while apical LS is lower in severe than moderate AS. Generally, apex measurements seem to be less accurate, with wider dispersion than the other LV levels. These echocardiographic findings may add to the conventional methods applied today in the work-up of patients with AS.

ACKNOWLEDGMENTS

The authors thank study nurse Liv Himle for her invaluable help in data acquisition. The authors have no funding sources to declare. This work was supported by The Bergesen Foundation, Oslo, and the Bergen University Heart Fund. The financial contributors played no part in the development or approval of this study.

CONFLICT OF INTEREST STATEMENT

The authors declare no conflicts of interest.

DATA AVAILABILITY STATEMENT

The data that support the findings of this study are available from the corresponding author upon reasonable request.

ORCID

Johannes Just Hjertaas MD, PhD  <https://orcid.org/0000-0002-4175-3303>

Sahrai Saeed MD, PhD  <https://orcid.org/0000-0003-4041-5019>

REFERENCES

1. Lorell BH, Carabello BA. Left ventricular hypertrophy: pathogenesis, detection, and prognosis. *Circulation*. 2000;102(4):470-479.
2. Rieck AE, Cramariuc D, Staal EM, Rossebo AB, Wachtell K, Gerdts E. Impact of hypertension on left ventricular structure in patients with asymptomatic aortic valve stenosis (a SEAS substudy). *J Hypertens*. 2010;28(2):377-383.
3. Saeed S, Gerdts E. Managing complications of hypertension in aortic valve stenosis patients. *Expert Rev Cardiovasc Ther*. 2018;16(12):897-907.
4. Singh A, Musa TA, Treibel TA, et al. Sex differences in left ventricular remodelling, myocardial fibrosis and mortality after aortic valve replacement. *Heart*. 2019;105(23):1818-1824.
5. Everett RJ, Tastet L, Clavel MA, et al. Progression of hypertrophy and myocardial fibrosis in aortic stenosis: a multicenter cardiac magnetic resonance study. *Circ Cardiovasc Imaging*. 2018;11(6):e007451.
6. Lee SP, Lee W, Lee JM, et al. Assessment of diffuse myocardial fibrosis by using MR imaging in asymptomatic patients with aortic stenosis. *Radiology*. 2015;274(2):359-369.

7. Cramariuc D, Gerdts E, Davidsen ES, Segadal L, Matre K. Myocardial deformation in aortic valve stenosis: relation to left ventricular geometry. *Heart*. 2010;96(2):106-112.
8. Ng AC, Delgado V, Bertini M, et al. Alterations in multidirectional myocardial functions in patients with aortic stenosis and preserved ejection fraction: a two-dimensional speckle tracking analysis. *Eur Heart J*. 2011;32(12):1542-1550.
9. Nagata Y, Takeuchi M, Wu VC, et al. Prognostic value of LV deformation parameters using 2D and 3D speckle-tracking echocardiography in asymptomatic patients with severe aortic stenosis and preserved LV ejection fraction. *JACC Cardiovasc Imaging*. 2015;8(3):235-245.
10. Ng ACT, Prihadi EA, Antoni ML, et al. Left ventricular global longitudinal strain is predictive of all-cause mortality independent of aortic stenosis severity and ejection fraction. *Eur Heart J Cardiovasc Imaging*. 2018;19(8):859-867.
11. Dahl JS, Magne J, Pellikka PA, Donal E, Marwick TH. Assessment of subclinical left ventricular dysfunction in aortic stenosis. *JACC Cardiovasc Imaging*. 2019;12(1):163-171.
12. Carstensen HG, Larsen LH, Hassager C, Kofoed KF, Jensen JS, Mogelvang R. Basal longitudinal strain predicts future aortic valve replacement in asymptomatic patients with aortic stenosis. *Eur Heart J Cardiovasc Imaging*. 2016;17(3):283-292.
13. Nagel E, Stuber M, Burkhard B, et al. Cardiac rotation and relaxation in patients with aortic valve stenosis. *Eur Heart J*. 2000;21(7):582-589.
14. Santoro A, Alvino F, Antonelli G, et al. Left ventricular twisting modifications in patients with left ventricular concentric hypertrophy at increasing after-load conditions. *Echocardiography*. 2014;31(10):1265-1273.
15. Parisi V, Losi MA, Contaldi C, et al. Speckle-tracking analysis based on 2D echocardiography does not reliably measure left ventricular torsion. *Clin Physiol Funct Imaging*. 2013;33(2):117-121.
16. Wu VC, Takeuchi M, Otani K, et al. Effect of through-plane and twisting motion on left ventricular strain calculation: direct comparison between two-dimensional and three-dimensional speckle-tracking echocardiography. *J Am Soc Echocardiogr*. 2013;26(11):1274-1281 e4.
17. Park CM, March K, Williams S, et al. Feasibility and reproducibility of left ventricular rotation by speckle tracking echocardiography in elderly individuals and the impact of different software. *PLoS One*. 2013;8(9):e75098.
18. Muraru D, Niero A, Rodriguez-Zanella H, Cherata D, Badano L. Three-dimensional speckle-tracking echocardiography: benefits and limitations of integrating myocardial mechanics with three-dimensional imaging. *Cardiovasc Diagn Ther*. 2018;8(1):101-117.
19. Holmes AA, Taub CC, Garcia MJ, Shan J, Slovut DP. Increased apical rotation in severe aortic stenosis is associated with reduced survival: a speckle-tracking study. *J Am Soc Echocardiogr*. 2015;28(11):1294-1301.
20. Tumenbayar M, Yamaguchi K, Yoshitomi H, Endo A, Tanabe K. Increased apical rotation in patients with severe aortic stenosis assessed by three-dimensional speckle tracking imaging. *J Echocardiogr*. 2018;16(1):28-33.
21. Musa TA, Uddin A, Swoboda PP, et al. Cardiovascular magnetic resonance evaluation of symptomatic severe aortic stenosis: association of circumferential myocardial strain and mortality. *J Cardiovasc Magn Reson*. 2017;19(1):13.
22. Hjertaas JJ, Fossa H, Dybdahl GL, Gruner R, Lunde P, Matre K. Accuracy of real-time single- and multi-beat 3-d speckle tracking echocardiography in vitro. *Ultrasound Med Biol*. 2013;39(6):1006-1014.
23. Hjertaas JJ, Matre K. A left ventricular phantom for 3D echocardiographic twist measurements. *Biomed Tech (Berl)*. 2020;65(2):209-218.
24. Lang RM, Badano LP, Mor-Avi V, et al. Recommendations for cardiac chamber quantification by echocardiography in adults: an update from the American Society of Echocardiography and the European Association of Cardiovascular Imaging. *J Am Soc Echocardiogr*. 2015;28(1):e14.
25. Otto CM, Nishimura RA, Bonow RO, et al. 2020 ACC/AHA Guideline for the Management of Patients With Valvular Heart Disease: a report of the American College of Cardiology/American Heart Association Joint Committee on Clinical Practice Guidelines. *Circulation*. 2021;143(5):e72-e227.
26. Vahanian A, Beyersdorf F, Praz F, et al. 2021 ESC/EACTS Guidelines for the management of valvular heart disease. *Eur Heart J*. 2021;43(7):561-632.
27. Nagueh SF, Smiseth OA, Appleton CP, et al. Recommendations for the evaluation of left ventricular diastolic function by echocardiography: an update from the American Society of Echocardiography and the European Association of Cardiovascular Imaging. *J Am Soc Echocardiogr*. 2016;29(4):277-314.
28. Attias D, Macron L, Dreyfus J, et al. Relationship between longitudinal strain and symptomatic status in aortic stenosis. *J Am Soc Echocardiogr*. 2013;26(8):868-874.
29. Schueler R, Sinning JM, Momcilovic D, et al. Three-dimensional speckle-tracking analysis of left ventricular function after transcatheter aortic valve implantation. *J Am Soc Echocardiogr*. 2012;25(8):827-834 e1.
30. van Dalen BM, Tzikas A, Soliman OI, et al. Left ventricular twist and untwist in aortic stenosis. *Int J Cardiol*. 2011;148(3):319-324.
31. Carasso S, Mutlak D, Lessick J, Reisner SA, Rakowski H, Agmon Y. Symptoms in severe aortic stenosis are associated with decreased compensatory circumferential myocardial mechanics. *J Am Soc Echocardiogr*. 2015;28(2):218-225.
32. Dahl JS, Videbaek L, Poulsen MK, Rudbaek TR, Pellikka PA, Moller JE. Global strain in severe aortic valve stenosis: relation to clinical outcome after aortic valve replacement. *Circ Cardiovasc Imaging*. 2012;5(5):613-620.
33. Vollema EM, Sugimoto T, Shen M, et al. Association of left ventricular global longitudinal strain with asymptomatic severe aortic stenosis: natural course and prognostic value. *JAMA Cardiol*. 2018;3(9):839-847.
34. Avila-Vanzini N, Fritche-Salazar JF, Vazquez-Castro NM, et al. Echocardiographic and histologic correlations in patients with severe aortic stenosis: influence of overweight and obesity. *J Cardiovasc Ultrasound*. 2016;24(4):303-311.
35. Ajmone Marsan N, Michalski B, Cameli M, et al. EACVI survey on standardization of cardiac chambers quantification by transthoracic echocardiography. *Eur Heart J Cardiovasc Imaging*. 2020;21(2):119-123.
36. Yodwut C, Weinert L, Klas B, Lang RM, Mor-Avi V. Effects of frame rate on three-dimensional speckle-tracking-based measurements of myocardial deformation. *J Am Soc Echocardiogr*. 2012;25(9):978-985.
37. Castano A, Narotsky DL, Hamid N, et al. Unveiling transthyretin cardiac amyloidosis and its predictors among elderly patients with severe aortic stenosis undergoing transcatheter aortic valve replacement. *Eur Heart J*. 2017;38(38):2879-2887.
38. Galat A, Guellich A, Bodez D, et al. Aortic stenosis and transthyretin cardiac amyloidosis: the chicken or the egg? *Eur Heart J*. 2016;37(47):3525-3531.
39. Phelan D, Collier P, Thavendiranathan P, et al. Relative apical sparing of longitudinal strain using two-dimensional speckle-tracking echocardiography is both sensitive and specific for the diagnosis of cardiac amyloidosis. *Heart*. 2012;98(19):1442-1448.
40. Dahl Pedersen AL, Povlsen JA, Dybro A, et al. Prevalence and prognostic implications of increased apical-to-basal strain ratio in patients with aortic stenosis undergoing transcatheter aortic valve replacement. *J Am Soc Echocardiogr*. 2020;33(12):1465-1473.

41. Saito M, Imai M, Wake D, et al. Prognostic assessment of relative apical sparing pattern of longitudinal strain for severe aortic valve stenosis. *Int J Cardiol Heart Vasc*. 2020;29:100551.
42. Badano LP, Cucchini U, Muraru D, Al Nono O, Sarais C, Illiceto S. Use of three-dimensional speckle tracking to assess left ventricular myocardial mechanics: inter-vendor consistency and reproducibility of strain measurements. *Eur Heart J Cardiovasc Imaging*. 2013;14(3):285-293.
43. Taylor RJ, Moody WE, Umar F, et al. Myocardial strain measurement with feature-tracking cardiovascular magnetic resonance: normal values. *Eur Heart J Cardiovasc Imaging*. 2015;16(8):871-881.
44. Andre F, Steen H, Matheis P, et al. Age- and gender-related normal left ventricular deformation assessed by cardiovascular magnetic resonance feature tracking. *J Cardiovasc Magn Reson*. 2015;17:25.

SUPPORTING INFORMATION

Additional supporting information can be found online in the Supporting Information section at the end of this article.

How to cite this article: Hjertaas JJ, Einarsen E, Gerdtts E, et al. Impact of aortic valve stenosis on myocardial deformation in different left ventricular levels: A three-dimensional speckle tracking echocardiography study. *Echocardiography*. 2023;1-12. [10.1111/echo.15668](https://doi.org/10.1111/echo.15668)